

Driver Drowsiness Estimation From EEG Signals Using Online Weighted Adaptation Regularization for Regression (OwARR)

Dongrui Wu ¹, Senior Member, IEEE, Vernon J. Lawhern, Member, IEEE, Stephen Gordon, Brent J. Lance, Senior Member, IEEE, and Chin-Teng Lin, Fellow, IEEE

Abstract—One big challenge that hinders the transition of brain–computer interfaces (BCIs) from laboratory settings to real-life applications is the availability of high-performance and robust learning algorithms that can effectively handle individual differences, i.e., algorithms that can be applied to a new subject with zero or very little subject-specific calibration data. Transfer learning and domain adaptation have been extensively used for this purpose. However, most previous works focused on classification problems. This paper considers an important regression problem in BCI, namely, online driver drowsiness estimation from EEG signals. By integrating fuzzy sets with domain adaptation, we propose a novel online weighted adaptation regularization for regression (OwARR) algorithm to reduce the amount of subject-specific calibration data, and also a source domain selection (SDS) approach to save about half of the computational cost of OwARR. Using a simulated driving dataset with 15 subjects, we show that OwARR and OwARR-SDS can achieve significantly smaller estimation errors than several other approaches. We also provide comprehensive analyses on the robustness of OwARR and OwARR-SDS.

Index Terms—Brain–computer interface, domain adaptation (DA), EEG, ensemble learning, fuzzy sets (FSs), transfer learning (TL).

I. INTRODUCTION

BRAIN–COMPUTER interfaces (BCIs) [18], [28], [32], [45], [53] have attracted rapidly increasing research

Manuscript received March 1, 2016; revised June 25, 2016; accepted October 2, 2016. Date of publication November 29, 2017; date of current version November 29, 2017. This research was supported by the U.S. Army Research Laboratory and was accomplished under Cooperative Agreement Numbers W911NF-10-2-0022 and W911NF-10-D-0002/TO 0023. It was also partially supported by the Australian Research Council (ARC) under discovery grant DP150101645.

D. Wu is with DataNova, Clifton Park, NY 12065 USA (e-mail: drwu09@gmail.com).

V. J. Lawhern is with the Human Research and Engineering Directorate, U.S. Army Research Laboratory, Aberdeen Proving Ground, Adelphi, MD 20783 USA, and also with the Department of Computer Science, University of Texas at San Antonio, San Antonio, TX 78249 USA (e-mail: vernon.j.lawhern.civ@mail.mil).

S. Gordon is with the DCS Corp, Alexandria, VA 22315 USA (e-mail: sgordon@dcsCorp.com).

B. J. Lance is with the Human Research and Engineering Directorate, U.S. Army Research Laboratory, Aberdeen Proving Ground, Aberdeen, MD 21005 USA (e-mail: brent.j.lance.civ@mail.mil).

C.-T. Lin is with the Faculty of Engineering and Information Technology, University of Technology Sydney, Sydney, NSW 2007, Australia, and also with the Brain Research Center, National Chiao-Tung University, Hsinchu 300, Taiwan (e-mail: Chin-Teng.Lin@uts.edu.au).

Color versions of one or more of the figures in this paper are available online at <http://ieeexplore.ieee.org>.

Digital Object Identifier 10.1109/TFUZZ.2016.2633379

interest in the last decade, thanks to recent advances in neurosciences, wearable/mobile biosensors, and analytics. However, there are still many challenges in their transition from laboratory settings to real-life applications, including the reliability and convenience of the sensing hardware [21], and the availability of high-performance and robust algorithms for signal analysis and interpretation that can effectively handle individual differences and nonstationarity [12], [25], [28], [50]. This paper focuses on the last challenge, more specifically, how to generalize a BCI algorithm to a new subject, with zero or very little subject-specific calibration data.

Transfer learning (TL) [34], which improves learning in a new task by leveraging data or knowledge from other relevant tasks, represents a promising solution to the above challenge. Many TL approaches have been proposed for BCI applications [50], including the following.

- 1) *Feature representation transfer* [7], [13], [39], [41]: It encodes the knowledge across different tasks as features.
- 2) *Instance transfer* [19], [20], [56], [63]: It uses certain parts of the data from other tasks to help the learning for the current task.
- 3) *Classifier transfer*: It includes domain adaptation (DA) [1], [41], [47], ensemble learning [42], [43], and their combinations [54], [60], [61].

However, most of the above TL approaches consider only BCI classification problems. Reducing the calibration data requirement in BCI regression problems has been largely understudied. One example is online driver drowsiness estimation from EEG signals, which will be investigated in this paper. This is a very important problem because drowsy driving is among the most important causes of road crashes, following only to alcohol, speeding, and inattention [38]. According to the National Highway Traffic Safety Administration [44], 2.5% of fatal motor vehicle crashes (on average 886/year in the U.S.) and 2.5% of fatalities (on average 1004/year in the U.S.) between 2005 and 2009 involved drowsy driving. However, to our best knowledge, there have been only two works [51], [54] on TL for drowsiness estimation. Wei *et al.* [51] showed that selective TL, which selectively turns TL on or off based the level of session generalizability, can achieve better estimation performance than approaches that always turn TL on or off. Wu *et al.* [54] proposed a DA with model fusion (DAMF) approach for drowsiness estimation. By making use of data from

other subjects in a DA framework, DAMF requires very little subject-specific calibration data, which significantly increases its real-world applicability.

In this paper, by making use of fuzzy sets (FSs) [67], we extend our earlier work on online weighted adaptation regularization (OwAR) [60] from classification to regression to estimate driver drowsiness online from EEG signals. We show that the two proposed algorithms can achieve significantly better estimation performance than the DAMF and two other baseline approaches.

The remainder of the paper is organized as follows. Section II introduces the details of the proposed online weighted adaptation regularization for regression (OwARR) algorithm. Section III further introduces a source domain selection (SDS) approach to save the computational cost of OwARR. Section IV presents experimental results and performance comparisons of OwARR and OwARR-SDS with three other approaches. Finally, Section V draws conclusions and points out future research directions.

II. ONLINE WEIGHTED ADAPTATION REGULARIZATION FOR REGRESSION

In [60], we have defined two types of calibration in BCI.

- 1) *Offline calibration*, in which a pool of unlabeled EEG epochs have been obtained *a priori*, and a subject or an oracle is queried to label some of these epochs, which are then used to train a model to label the remaining epochs in the pool.
- 2) *Online calibration*, in which some labeled EEG epochs are obtained on-the-fly, and then a model is trained from them for future (unseen) EEG epochs.

The major different between them is that, for offline calibration, the unlabeled EEG epochs can be used to help design the model (e.g., semisupervised learning), whereas in online calibration there are no unlabeled EEG epochs. Additionally, in offline calibration we can query any epoch in the pool for the label, but in online calibration usually the sequence of the epochs is predetermined and the subject or oracle has little control on which epochs to see next.

We only consider online calibration in this paper. This section introduces the OwARR algorithm, which extends the OwAR algorithm [60] from classification to regression, by making use of FSs.

A. Problem Definition

A domain [23], [34] \mathcal{D} in TL consists of a d -dimensional feature space \mathcal{X} and a marginal probability distribution $P(\mathbf{x})$, i.e., $\mathcal{D} = \{\mathcal{X}, P(\mathbf{x})\}$, where $\mathbf{x} \in \mathcal{X}$. Two domains \mathcal{D}^z and \mathcal{D}^t are different if $\mathcal{X}^z \neq \mathcal{X}^t$, and/or $P^z(\mathbf{x}) \neq P^t(\mathbf{x})$.

A task [23], [34] \mathcal{T} in TL consists of an output space \mathcal{Y} and a conditional probability distribution $Q(y|\mathbf{x})$. Two tasks \mathcal{T}^z and \mathcal{T}^t are different if $\mathcal{Y}^z \neq \mathcal{Y}^t$, or $Q^z(y|\mathbf{x}) \neq Q^t(y|\mathbf{x})$.

Given the z th source domain \mathcal{D}^z with n_z samples (\mathbf{x}_i^z, y_i^z) , $i = 1, \dots, n_z$, and a target domain \mathcal{D}^t with m calibration samples (\mathbf{x}_j^t, y_j^t) , $j = 1, \dots, m$, DA aims to learn a target prediction function $f(\mathbf{x}) : \mathbf{x} \mapsto y$ with low expected error on \mathcal{D}^t , under

the assumptions that $\mathcal{X}^z = \mathcal{X}^t$, $\mathcal{Y}^z = \mathcal{Y}^t$, $P^z(\mathbf{x}) \neq P^t(\mathbf{x})$, and $Q^z(y|\mathbf{x}) \neq Q^t(y|\mathbf{x})$.

In driver drowsiness estimation from EEG signals, EEG signals from a new subject are in the target domain, while EEG signals from the z th existing subject are in the z th source domain. A single data sample consists of the feature vector for a single EEG epoch in either domain. Although the features in source and target domains are extracted in the same way, generally their marginal and conditional probability distributions are different, i.e., $P^z(\mathbf{x}) \neq P^t(\mathbf{x})$ and $Q^z(y|\mathbf{x}) \neq Q^t(y|\mathbf{x})$, because different subjects usually have similar but distinct drowsy neural responses. As a result, data from a source domain cannot represent data in the target domain accurately, and must be integrated with some target domain data to induce the target domain regression function.

B. Learning Framework

Because

$$f(\mathbf{x}) = Q(y|\mathbf{x}) = \frac{P(\mathbf{x}, y)}{P(\mathbf{x})} = \frac{Q(\mathbf{x}|y)P(y)}{P(\mathbf{x})} \quad (1)$$

to use the data in the z th source domain in the target domain, we need to minimize the distance between the marginal and conditional probability distributions in the two domains by ensuring that¹ $P^z(\mathbf{x})$ is close to $P^t(\mathbf{x})$, and $Q^z(\mathbf{x}|y)$ is also close to $Q^t(\mathbf{x}|y)$.

Assume both the output and each dimension of the input vector have zero mean. Then, the regression function can be written as

$$f(\mathbf{x}) = \boldsymbol{\alpha}^T \mathbf{x} \quad (2)$$

where $\boldsymbol{\alpha}$ is the regression parameter vector to be found. The learning framework of OwARR is then formulated as

$$f = \arg \min_f \sum_{i=1}^n (y_i - f(\mathbf{x}_i))^2 + w^t \sum_{i=n+1}^{n+m} (y_i - f(\mathbf{x}_i))^2 + \lambda[d(P^z, P^t) + d(Q^z, Q^t)] - \gamma \tilde{r}^2(y, f(\mathbf{x})) \quad (3)$$

where λ and γ are nonnegative regularization parameters, and w^t is the overall weight for target domain samples, which should be larger than 1 so that more emphasis is given to target domain samples than source domain samples.

Briefly speaking, the first two terms in (3) minimize the sum of squared errors in the source domain and target domain, respectively. The third term minimizes the distance between the marginal and conditional probability distributions in the two domains. The last term maximizes the approximate sample Pearson's correlation coefficient between y and $f(\mathbf{x})$, which helps avoid the undesirable situation that the regression output is (nearly) a constant.

In the following sections, we will explain how to compute the individual terms in (3).

¹Strictly speaking, we should also make sure $P^z(y)$ is close to $P^t(y)$. In this paper, we assume $P^z(y)$ and $P^t(y)$ are close. Our future research will consider the general case that $P^z(y)$ and $P^t(y)$ are different.

C. Sum of Squared Error Minimization

Let

$$X = [\mathbf{x}_1, \dots, \mathbf{x}_{n+m}]^T \quad (4)$$

$$\mathbf{y} = [y_1, \dots, y_{n+m}]^T \quad (5)$$

where the first n \mathbf{x}_i and y_i are the column input vectors and the corresponding outputs in the source domain, the next m \mathbf{x}_i and y_i are the column input vectors and the corresponding outputs in the target domain, and T is the matrix transpose operation.

Define $E \in R^{(n+m) \times (n+m)}$ as a diagonal matrix with

$$E_{ii} = \begin{cases} 1, & 1 \leq i \leq n \\ w^t, & n+1 \leq i \leq n+m. \end{cases} \quad (6)$$

Then, the first two terms in (3) can be rewritten as

$$\begin{aligned} & \sum_{i=1}^n (y_i - f(\mathbf{x}_i))^2 + w^t \sum_{i=n+1}^{n+m} (y_i - f(\mathbf{x}_i))^2 \\ &= \sum_{i=1}^{n+m} E_{ii} (y_i - \alpha^T \mathbf{x}_i)^2 \\ &= (\mathbf{y}^T - \alpha^T X^T) E (\mathbf{y} - X \alpha). \end{aligned} \quad (7)$$

The optimal selection of w^t is very important to the performance of the OwARR algorithm. In this paper, we use

$$w^t = \max(2, \sigma \cdot n/m) \quad (8)$$

where σ is a positive adjustable parameter, based on the following heuristics.

- 1) When m is small, each target domain sample should have a large weight so that the target domain is not overwhelmed by the source domain.
- 2) As m increases, the weight on the target domain samples should decrease gradually so that the source domain is not overwhelmed by the target domain.
- 3) The target domain samples should always have larger weights than the source domain samples because eventually the regression model will be applied to the target domain.

D. Marginal Probability Distribution Adaptation

As in [23], [36], [60], and [61], we compute $d(P^z, P^t)$ using the maximum mean discrepancy (MMD):

$$\begin{aligned} d(P^z, P^t) &= \left[\frac{1}{n} \sum_{i=1}^n f(\mathbf{x}_i) - \frac{1}{m} \sum_{i=n+1}^{n+m} f(\mathbf{x}_i) \right]^2 \\ &= \alpha^T X M_P X \alpha \end{aligned} \quad (9)$$

where $M_P \in R^{(n+m) \times (n+m)}$ is the MMD matrix given as

$$(M_P)_{ij} = \begin{cases} \frac{1}{n^2}, & 1 \leq i \leq n, 1 \leq j \leq n \\ \frac{1}{m^2}, & n+1 \leq i \leq n+m, \\ & n+1 \leq j \leq n+m \\ -\frac{1}{nm}, & \text{otherwise} \end{cases} \quad (10)$$

E. Conditional Probability Distribution Adaptation

In [23], [60], and [61], a classification problem is considered, and it is more straightforward to perform conditional probability distribution adaptation. In this section, we first briefly introduce the technique used there, and then describe in detail how we can perform conditional probability distribution adaptation in regression in a similar way, with the help of FSs [16], [67], which have been widely used in EEG feature extraction [5], [15], [24] and pattern recognition [11], [22], [33].

1) *Conditional Probability Distribution Adaptation for Classification*: Let $\mathcal{D}_c^z = \{\mathbf{x}_i | \mathbf{x}_i \in \mathcal{D}^z \wedge y_i = c\}$ be the set of samples in Class c ($c = 1, \dots, C$) of the z th source domain, $\mathcal{D}_c^t = \{\mathbf{x}_i | \mathbf{x}_i \in \mathcal{D}^t \wedge y_i = c\}$ be the set of samples in Class c of the target domains, $n_c = |\mathcal{D}_c^z|$ and $m_c = |\mathcal{D}_c^t|$. Then, the distance between the conditional probability distributions in source and target domains is computed as the sum of the Euclidian distances between the class means in the two domains [23], [60], [61], i.e.,

$$d(Q^z, Q^t) = \sum_{c=1}^C \left[\frac{1}{n_c} \sum_{\mathbf{x}_i \in \mathcal{D}_c^z} f(\mathbf{x}_i) - \frac{1}{m_c} \sum_{\mathbf{x}_i \in \mathcal{D}_c^t} f(\mathbf{x}_i) \right]^2. \quad (11)$$

2) *Conditional Probability Distribution Adaptation for Regression*: With the help of FSs (background materials are given in the Appendix), we can transform the regression problem into a ‘‘classification’’ problem and hence perform conditional probability distribution adaptation using (11). First, for the n_z outputs, $\{y_i^z\}_{i=1, \dots, n}$, in the z th source domain, we find their 5, 50, and 95 percentile² values, p_5^z , p_{50}^z and p_{95}^z , respectively, and define three triangular FSs³, Small^z, Medium^z, and Large^z, based on them, as shown in Fig. 1(a). In this way, we can ‘‘classify’’ the outputs in the z th source domain into three fuzzy classes, Small^z, Medium^z, and Large^z, corresponding to the different classes in a traditional crisp classification problem. However, note that in the traditional crisp classification problem a sample can only belong to one class. For the fuzzy classes here,

²There is a popular regression analysis method called quantile regression [17] in statistics and econometrics, which estimates either the conditional median or other quantiles of the response variable. The percentiles used in this paper are found directly from the data, and they should not be confused with quantile regression.

³There can be other ways to define these FSs, e.g., we could use Gaussian FSs instead of triangular FSs, use p_{10}^z , p_{50}^z , and p_{90}^z instead of p_5^z , p_{50}^z , and p_{95}^z , use other than three FSs in each domain, or use type-2 FSs [30] instead of type-1. Three type-1 triangular FSs are used here for simplicity. More discussions on the sensitivity of the OwARR algorithm to the number of type-1 triangular FSs are given in Section IV-H.

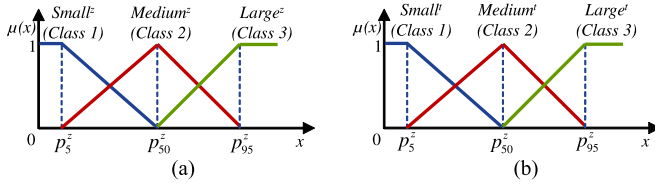


Fig. 1. Three FSs in the (a) z th source domain, and (b) target domain.

a sample can belong to more than one class simultaneously, at different degrees.

Denote Class Small z as Class 1, Class Medium z as Class 2, Class Large z as Class 3, and the membership degree of y_i^z in Class c as μ_{ic}^z . We then normalize each μ_{ic}^z according to its class, i.e.,

$$\bar{\mu}_{ic}^z = \frac{\mu_{ic}^z}{\sum_{i=1}^n \mu_{ic}^z}, \quad i = 1, \dots, n; \quad c = 1, 2, 3. \quad (12)$$

Similarly, we also find p_5^t , p_{50}^t , and p_{95}^t from the m target domain outputs $\{y_i^t\}_{i=n+1, \dots, n+m}$, define three FSs, Small t , Medium t , and Large t , as shown in Fig. 1(b), and compute the corresponding normalized $\bar{\mu}_{ic}^t$, $i = n+1, \dots, n+m$, $c = 1, 2, 3$.

Finally, similar to (11), the distance between the conditional probability distributions in the target domain and the z th source domain is computed as

$$d(Q^z, Q^t) = \sum_{c=1}^3 \left[\sum_{\mathbf{x}_i \in \mathcal{D}^z} \bar{\mu}_{ic}^z f(\mathbf{x}_i) - \sum_{\mathbf{x}_i \in \mathcal{D}^t} \bar{\mu}_{ic}^t f(\mathbf{x}_i) \right]^2. \quad (13)$$

Substituting (2) into (13), it follows that

$$\begin{aligned} d(Q^z, Q^t) &= \sum_{c=1}^3 \left[\sum_{\mathbf{x}_i \in \mathcal{D}^z} \bar{\mu}_{ic}^z \alpha^T \mathbf{x}_i - \sum_{\mathbf{x}_i \in \mathcal{D}^t} \bar{\mu}_{ic}^t \alpha^T \mathbf{x}_i \right]^2 \\ &= \sum_{c=1}^3 \alpha^T X M_c X \alpha = \alpha^T X M_Q X \alpha \end{aligned} \quad (14)$$

where

$$M_Q = M_1 + M_2 + M_3 \quad (15)$$

in which M_1 , M_2 , and M_3 are MMD matrices computed as

$$(M_c)_{ij} = \begin{cases} \bar{\mu}_{ic}^z \bar{\mu}_{jc}^z, & \mathbf{x}_i, \mathbf{x}_j \in \mathcal{D}_c^z \\ \bar{\mu}_{ic}^t \bar{\mu}_{jc}^t, & \mathbf{x}_i, \mathbf{x}_j \in \mathcal{D}_c^t \\ -\bar{\mu}_{ic}^z \bar{\mu}_{jc}^t, & \mathbf{x}_i \in \mathcal{D}_c^z, \mathbf{x}_j \in \mathcal{D}_c^t \\ -\bar{\mu}_{ic}^t \bar{\mu}_{jc}^z, & \mathbf{x}_i \in \mathcal{D}_c^t, \mathbf{x}_j \in \mathcal{D}_c^z \\ 0, & \text{otherwise} \end{cases}. \quad (16)$$

F. Maximize the Approximate Sample Pearson Correlation Coefficient

The sample Pearson correlation coefficient $r(y, f(\mathbf{x}))$ is defined as [48]

$$\begin{aligned} r(y, f(\mathbf{x})) &= \frac{\mathbf{y}^T X \alpha}{\|\mathbf{y}\| \cdot \|X \alpha\|} \\ &= \frac{\mathbf{y}^T X \alpha}{\sqrt{\mathbf{y}^T \mathbf{y}} \cdot \sqrt{\alpha^T X^T X \alpha}} \end{aligned} \quad (17)$$

and hence

$$r^2(y, f(\mathbf{x})) = \frac{\alpha^T X^T \mathbf{y} \mathbf{y}^T X \alpha}{\mathbf{y}^T \mathbf{y} \cdot \alpha^T X^T X \alpha}. \quad (18)$$

Note that $r^2(y, f(\mathbf{x}))$ has α in the denominator, so it is very challenging to find a closed-form solution to maximize it. However, observe that $r^2(y, f(\mathbf{x}))$ increases as $\alpha^T X^T \mathbf{y} \mathbf{y}^T X \alpha$ increases, and decreases as $\alpha^T X^T X \alpha$ increases. So, instead of maximizing $r^2(y, f(\mathbf{x}))$ directly, in this paper we try to maximize the following function:

$$\begin{aligned} \tilde{r}^2(y, f(\mathbf{x})) &= \frac{\alpha^T X^T \mathbf{y} \mathbf{y}^T X \alpha - \alpha^T X^T X \alpha}{\mathbf{y}^T \mathbf{y}} \\ &= \frac{\alpha^T X^T (\mathbf{y} \mathbf{y}^T - I) X \alpha}{\mathbf{y}^T \mathbf{y}} \end{aligned} \quad (19)$$

where $I \in R^{(n+m) \times (n+m)}$ is an identity matrix. $\tilde{r}^2(y, f(\mathbf{x}))$ has the same property as $r^2(y, f(\mathbf{x}))$, i.e., $\tilde{r}^2(y, f(\mathbf{x}))$ increases as $\alpha^T X^T \mathbf{y} \mathbf{y}^T X \alpha$ increases, and decreases as $\alpha^T X^T X \alpha$ increases.

G. Closed-Form Solution

Substituting (7), (9), (14), and (19) into (3), we can rewrite it as

$$\begin{aligned} \alpha &= \arg \min_{\alpha} (\mathbf{y}^T - \alpha^T X^T) E (\mathbf{y} - X \alpha) \\ &\quad + \lambda \alpha^T X^T (M_P + M_Q) X \alpha \\ &\quad + \gamma \frac{\alpha^T X^T (I - \mathbf{y} \mathbf{y}^T) X \alpha}{\mathbf{y}^T \mathbf{y}}. \end{aligned} \quad (20)$$

Setting the derivative of the objective function above to 0 leads to

$$\alpha = \left[X^T \left(E + \lambda M_P + \lambda M_Q + \gamma \frac{I - \mathbf{y} \mathbf{y}^T}{\mathbf{y}^T \mathbf{y}} \right) X \right]^{-1} X^T E \mathbf{y}. \quad (21)$$

H. Complete OwARR Algorithm

The pseudocode for the complete OwARR algorithm is described in Algorithm 1. We first perform OwARR for each source domain separately, and then construct the final regression model as a weighted average of these base models, where the weight is the inverse of the training accuracy of the corresponding base model. The final regression model will then be applied to future unlabeled data.

Algorithm1: The OwARR algorithm.

Input: Z source domains, where the z^{th} ($z = 1, \dots, Z$) domain has n_z samples $\{\mathbf{x}_i^z, y_i^z\}_{i=1, \dots, n_z}$; m target domain samples, $\{\mathbf{x}_j^t, y_j^t\}_{j=1, \dots, m}$; Parameters λ, γ , and σ in (8).

Output: The OwARR regression model.

for $z = 1, 2, \dots, Z$ **do**
 Construct X in (4), \mathbf{y} in (5), E in (6), M_P in (10), and M_Q in (15);
 Compute α by (21) and record it as α^z ;
 Use α^z to estimate the outputs for the $n_z + m$ samples from both domains and record the root mean squared error as a^z ;
 Assign the z^{th} regression model a weight $w^z = 1/a^z$;
end

Return $f(\mathbf{x}) = \frac{\sum_{z=1}^Z w^z (\alpha^z)^T \mathbf{x}}{\sum_{z=1}^Z w^z}$.

III. ONLINE WEIGHTED ADAPTATION REGULARIZATION FOR REGRESSION SOURCE DOMAIN SELECTION

An SDS procedure for online classification problems has been proposed in [60]. In this paper, it is extended to regression problems by using the fuzzy classes again defined in Fig. 1. The primary goal of SDS is to reduce the computational cost of OwARR, because when there is a large number of source domains, performing OwARR for each source domain and then aggregating the base models would be very time consuming.

Assume there are Z different source domains. For the z^{th} source domain, we first compute \mathbf{m}_c^z ($c = 1, 2, 3$), the mean vector of each fuzzy class. Then, we also compute \mathbf{m}_c^t , the mean vector of each fuzzy class in the target domain, from the m labeled samples. The distance between the two domains is

$$d(z, t) = \sum_{c=1}^3 \|\mathbf{m}_c^z - \mathbf{m}_c^t\|. \quad (22)$$

We next cluster the Z numbers, $\{d(z, t)\}_{z=1, \dots, Z}$, by k -means clustering, and finally choose the cluster that has the smallest centroid, i.e., the source domains that are closest to the target domain. In this way, on average we only need to perform OwARR for Z/k source domains. We used $k = 2$ in this paper.

The pseudocode for the complete OwARR-SDS algorithm is described in Algorithm 2. We first use SDS to select the Z' closest source domains, and then perform DA for each selected source domain separately. The final regression model is a weighted average of these base models, with the weight being the inverse of the training accuracy of the corresponding base model.

IV. EXPERIMENTS AND DISCUSSIONS

Experimental results on driver drowsiness estimation from EEG signals are presented in this section to demonstrate the performance of OwARR and OwARR-SDS.

Algorithm2: The OwARR-SDS algorithm.

Input: Z source domains, where the z^{th} ($z = 1, \dots, Z$) domain has n_z samples $\{\mathbf{x}_i^z, y_i^z\}_{i=1, \dots, n_z}$; m target domain samples, $\{\mathbf{x}_j^t, y_j^t\}_{j=1, \dots, m}$; λ, γ, σ in (8), and k in k -means clustering.

Output: The OwARR-SDS regression model.

// SDS starts

if $m == 0$ **then**
 Select all Z source domains;
 Go to OwARR.
else
for $z = 1, 2, \dots, Z$ **do**
 Compute $d(z, t)$, the distance between the target domain and the z^{th} source domain, by (22).
end
 Cluster $\{d(z, t)\}_{z=1, \dots, Z}$ by k -means clustering;
 Select the Z' source domains that belong to the cluster with the smallest centroid.
end

// SDS ends; OwARR starts

for $z = 1, 2, \dots, Z'$ **do**
 Construct X in (4), \mathbf{y} in (5), E in (6), M_P in (10), and M_Q in (15);
 Compute α by (21) and record it as α^z ;
 Use α^z to estimate the outputs for the $n_z + m$ samples from both domains and record the root mean squared error as a^z ;
 Assign the z^{th} regression model a weight $w^z = 1/a^z$;
end

// OwARR ends

Return $f(\mathbf{x}) = \frac{\sum_{z=1}^{Z'} w^z (\alpha^z)^T \mathbf{x}}{\sum_{z=1}^{Z'} w^z}$.

A. Experiment Setup

We reused the experiment setup and data mentioned in [54]. Sixteen healthy subjects with normal or corrected to normal vision were recruited to participate in a sustained-attention driving experiment [3], [4], which consisted of a real vehicle mounted on a motion platform with 6 degrees of freedom immersed in a 360° virtual reality scene. Each participant read and signed an informed consent form before the experiment began. Each experiment lasted for about 60–90 min and was conducted in the afternoon when the circadian rhythm of sleepiness reached its peak. To induce drowsiness during driving, the virtual reality scenes simulated monotonous driving at a fixed 100 km/h speed on a straight and empty highway. During the experiment, lane-departure events were randomly applied every 5–10 s, and participants were instructed to steer the vehicle to compensate for these perturbations as quickly as possible. Subjects' cognitive states and driving performance were monitored via a surveillance video camera and the vehicle trajectory throughout the experiment. The response time in response to the perturbation was recorded and later converted to drowsiness index. Meanwhile, participants' scalp EEG signals were recorded using a 32-channel (30-channel EEGs plus 2-channel earlobes) 500 Hz Neuroscan NuAmps Express system (Compumedics Ltd., VIC, Australia).

The Institutional Review Board of the Taipei Veterans General Hospital approved the experimental protocol.

B. Evaluation Process and Performance Measures

The complete procedure for the application of OwARR for driver drowsiness estimation is given in Algorithm 3. Compared with Algorithm 1 on OwARR for a generic application, here we also include detailed EEG data preprocessing and feature extraction steps. Observe that although the feature extraction methods for different auxiliary subjects have the same steps, their parameters (channels removed, principal components (PCs) used, ranges used in normalization) may be different, so we need to record them for each auxiliary subject so that the features in the individual regression models can be computed correctly.

From the experiments, we already knew the drowsiness indices for all ~ 1200 epochs. To evaluate the performances of different algorithms, for each subject, we used up to 100 epochs in a randomly chosen continuous block for calibration, and the rest ~ 1100 epochs for testing. Every time when five epochs were acquired, we computed the testing performance to show how the performance of the regression models changed over time. We ran this evaluation process 30 times, each time with a randomly chosen 100-epoch calibration block, to obtain statistically meaningful results. Finally, we repeated this entire process 15 times so that each subject had a chance to be the “15th” subject.

The primary performance measured used in this paper is the root-mean-squared error (RMSE) between the ~ 1100 true drowsiness indices and the corresponding estimates for the testing epochs, which is optimized in the object functions of all algorithms. The secondary performance measure is the correlation coefficient (CC) between the true drowsiness indices and the estimates.

C. Preprocessing and Feature Extraction

The 16 subjects had different lengths of experiment, because the disturbances were presented randomly every 5–10 s. Data from one subject were not correctly recorded, so we used only 15 subjects. To ensure fair comparison, we used only the first 3600 s data for each subject.

We defined a function [51], [54] to map the response time τ to a drowsiness index $y \in [0, 1]$:

$$y = \max \left\{ 0, \frac{1 - e^{-(\tau - \tau_0)}}{1 + e^{-(\tau - \tau_0)}} \right\}, \quad (23)$$

$\tau_0 = 1$ was used in this paper, as in [54]. The drowsiness indices were then smoothed using a 90-s square moving-average window to reduce variations. This does not reduce the sensitivity of the drowsiness index because the cycle lengths of drowsiness fluctuations are longer than 4 min [26]. The smoothed drowsiness indices for the 15 subjects are shown in Fig. 2. Observe that each subject had some drowsiness indices at or close to 1, indicating drowsy driving.

We used EEGLAB [6] for EEG signal preprocessing. A band-pass filter (1–50 Hz) was applied to remove high-frequency muscle artifacts, line-noise contamination and dc drift. Next,

Algorithm3: OwARR for driver drowsiness estimation.

Input: EEG data and the corresponding RTs;
 λ , γ , and σ in OwARR (Algorithm 2);
 t_{\max} , the duration of the calibration period;
 Δt , the time interval (in second) between two successive epochs in calibration.
Output: The OwARR regression model.
Set $t = 0$, and start the calibration;
while $t < t_{\max}$ **do**
 if $t \geq 30$ **then**
 Compute the drowsiness index y in (5);
 // Pre-processing
 Extract 30s EEG data in $[t - 30, t]$;
 Band-pass filter the EEG signals to $[0, 50]$ Hz;
 Down-sample to 250Hz;
 Re-reference to averaged earlobes;
 Compute the PSD in the $[4, 7.5]$ Hz theta band for each channel;
 Convert the PSDs to dB for each channel;
 end
 Wait until $t = t + \Delta t$;
end
// OwARR
for $z = 1, 2, \dots, Z$ **do**
 // Feature extraction
 Concatenate each channel of the powers of the z^{th} subject with the corresponding powers of the new subject;
 Remove channels which have at least one power larger than a certain threshold;
 Normalize the powers of each remaining channel to mean 0 and std 1;
 Put all the powers in a matrix, whose rows represent different EEG channels;
 Extract a few leading principal components of the power matrix that account for 95% of the variance;
 Find the corresponding scores of the leading principal components;
 Normalize each dimension of the scores to $[0, 1]$;
 Collect the scores for each epoch as features;
 Record the parameters of the feature extraction method (channels removed, principal components used, ranges used in normalization) as FE^z ;
 // OwARR training
 Construct X in (4), y in (5), E in (6), M_P in (10), and M_Q in (15);
 Compute α by (21) and record it as α^z ;
 Use α^z to estimate the outputs for all known samples and record the root mean squared error as a^z ;
 Assign the z^{th} regression model a weight $w^z = 1/a^z$;
end
Return The OwARR regression model
 $f(\mathbf{x}) = \frac{\sum_{z=1}^Z w^z (\alpha^z)^T \mathbf{x}^z}{\sum_{z=1}^Z w^z}$, where \mathbf{x}^z is the feature vector extracted using FE^z .

the EEG data were downsampled from 500 to 250 Hz and rereferenced to averaged earlobes.

We tried to predict the drowsiness index for each subject every 3 s. All 30 EEG channels were used in feature extraction. We epoched 30-s EEG signals right before each sample point,

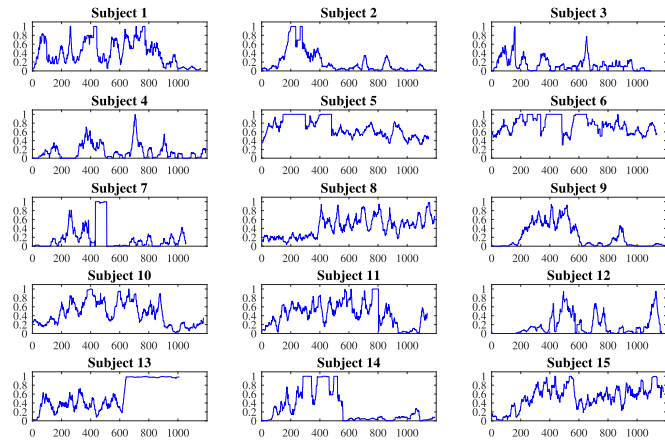


Fig. 2. Drowsiness indices of the 15 subjects.

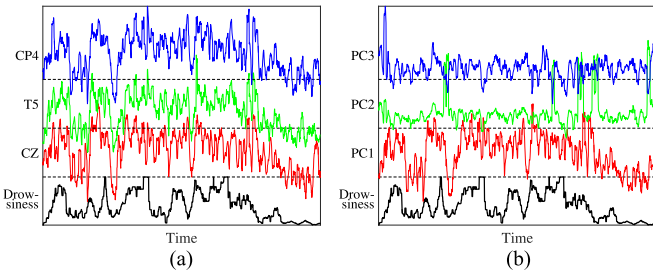


Fig. 3. EEG features and the corresponding drowsiness indices for Subject 1. (a) Theta band powers for three selected channels and (b) top three PC features.

and computed the average power spectral density (PSD) in the theta band (4–7.5 Hz) for each channel using Welch’s method [52], as research [27] has shown that theta band spectrum is a strong indicator of drowsiness. The theta band powers for three selected channels and the corresponding drowsiness index for Subject 1 are shown in Fig. 3(a). Observe that drowsiness index has strong correlations with the theta band powers.

Next, we converted the 30 theta band powers to dBs. To remove noises or bad channel readings, we removed channels whose maximum dBs were larger than 20. We then normalized the dBs of each remaining channel to mean zero and standard deviation one, and extracted a few (usually around 10) leading PC, which accounted for 95% of the variance. The projections of the theta band powers onto these PCs were then normalized to $[0, 1]$ and used as our features. Three such features for Subject 1 are shown in Fig. 3(b). Observe that the score on the first PC has obvious correlation with the drowsiness index, suggesting that estimating the drowsiness index from the scores on the PCs is possible.

D. Algorithms

We compared the performances of OwARR and OwARR-SDS with three other algorithms introduced in [54].

- 1) Baseline 1 (BL1), which combines data from all 14 existing subjects, builds a ridge regression model [10], and applies it to the new subject. That is, BL1 tries to build a subject-independent regression model and ignores data from the new subject completely.

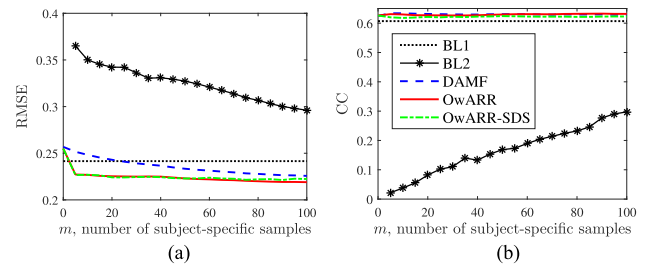


Fig. 4. Average performances of the five algorithms across the 15 subjects. (a) RMSE and (b) CC.

- 2) Baseline 2 (BL2), which builds a ridge regression model using only subject-specific calibration samples from the new subject. That is, BL2 ignores data from existing subjects completely.
- 3) DAMF, which builds 14 ridge regression models by combining data from each auxiliary subject with data from the new subject, respectively, and then uses a weighted average to obtain the final regression model. The weights are also the inverse of the training RMSEs, as in Algorithms 1 and 2.

The ridge parameter $\sigma = 0.01$ was used in the above three algorithms, as in [54]. For OwARR and OwARR-SDS, we used $\sigma = 0.2$, $\lambda = 10$, and $\gamma = 0.5$. However, as will be shown in Section IV-H, OwARR and OwARR-SDS are robust to these three parameters.

E. Regression Performance Comparison

The average RMSEs and CCs for the 5 algorithms across the 15 subjects are shown in Fig. 4, and the RMSEs and CCs for the individual subjects are shown in Fig. 5. Observe that DAMF, OwARR, and OwARR-SDS had very similar CCs, and all of them were better than the CCs of BL1 and BL2. Additionally, they exhibited the following characteristics.

- 1) Except for BL1, whose model does not depend on m , all the other four algorithms gave smaller RMSEs as m increased, which is intuitive.
- 2) BL1 had the smallest RMSE when $m = 0$. However, as m increased, DAMF, OwARR, and OwARR-SDS quickly outperformed BL1. This suggests that there is large individual difference among the subjects, and hence a subject-independent model is not desirable.
- 3) Because BL2 used only subject-specific calibration data, it cannot build a model when $m = 0$, i.e., when there was no subject-specific calibration data at all. However, all the other four methods can, because they can make use of data from other subjects. BL2’s performance was the worst, because it cannot get enough training when there is only a small number of subject-specific calibration samples.
- 4) OwARR and OwARR-SDS had almost identical average RMSEs, which were smaller than those of BL1, BL2, and DAMF. More importantly, the RMSEs of OwARR and OwARR-SDS almost converged as soon as the first batch of subject-specific samples were added, suggesting that they only need very few subject-specific samples to train, which is very desirable in practical calibration.

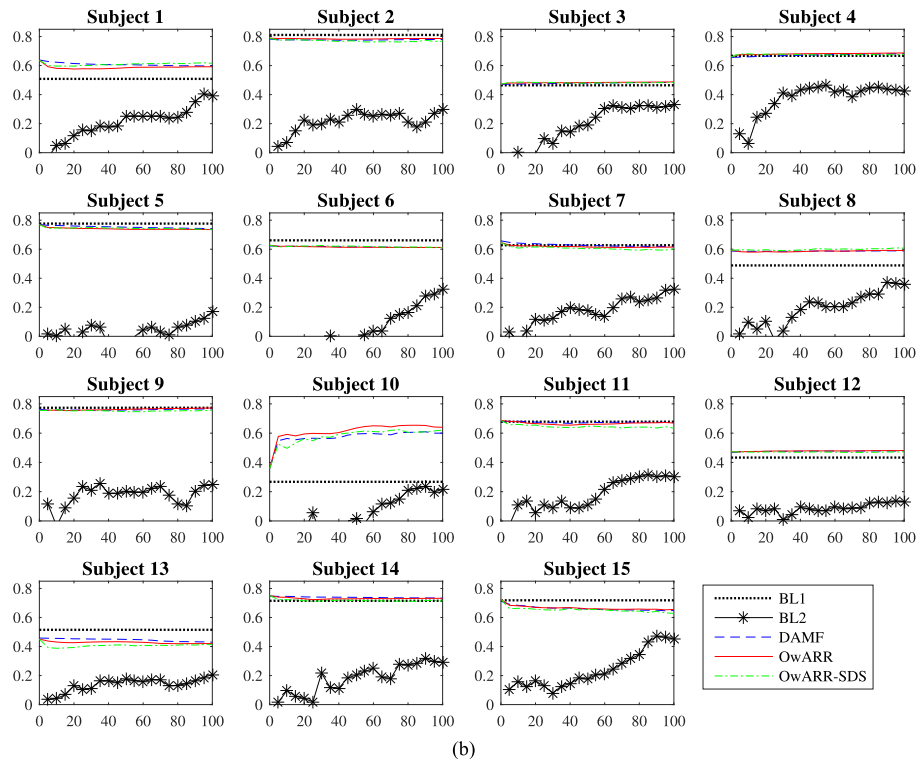
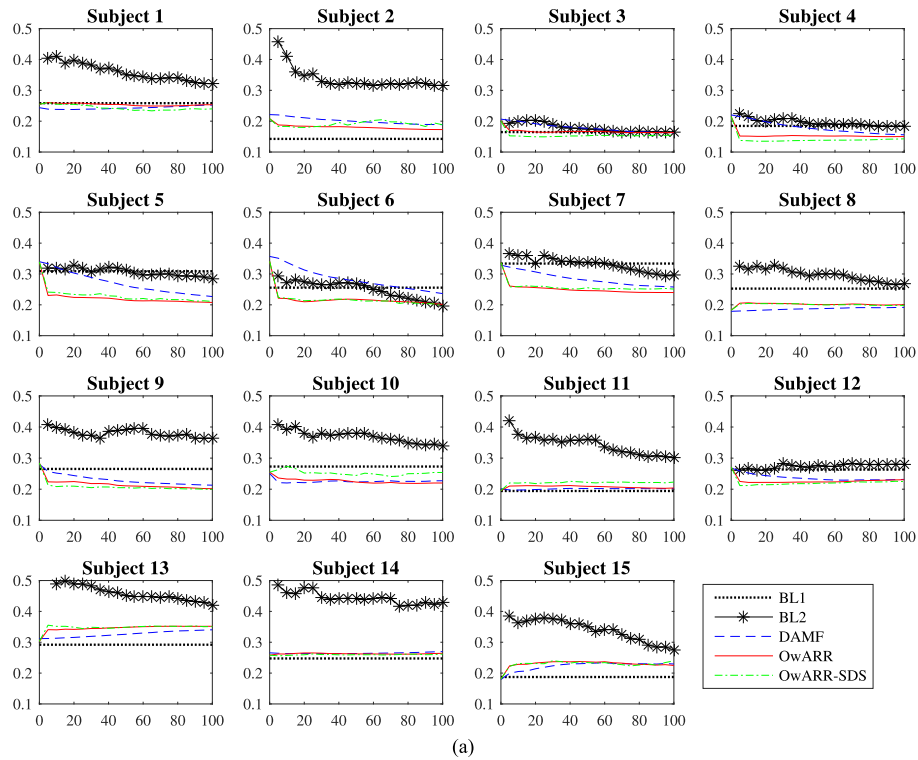


Fig. 5. Average performances of the five algorithms for each individual subject. Horizontal axis: m , the number of subject-specific calibration samples. (a) RMSE and (b) CC.

In summary, the three DA-based approaches generally had better performance than BL1, which does not use subject-specific data at all, and also BL2, which does not use auxiliary data at all. This suggests that DA is indeed beneficial. Moreover, our proposed OwARR and OwARR-SDS achieved the best overall performances among the five algorithms.

We also performed two-way Analysis of Variance (ANOVA) for each m to check if the RMSE differences among the five algorithms were statistically significant, by setting the subjects as a random effect. Two-way ANOVA showed statistically significant differences among them ($p < 0.01$) for all m . Then, nonparametric multiple comparison tests using Dunn's

TABLE I
 p -VALUES OF NONPARAMETRIC MULTIPLE COMPARISONS

m	OwARR versus BL1	OwARR versus BL2	OwARR versus DAMF	OwARR-SDS versus BL1	OwARR-SDS versus BL2	OwARR-SDS versus DAMF	OwARR-SDS versus OwARR
0	.0007	N/A	.4073	.0011	N/A	.5091	.5000
5	.0000	.0000	.0000	.0000	.0000	.0000	.4813
10	.0000	.0000	.0000	.0000	.0000	.0000	.3888
15	.0000	.0000	.0000	.0000	.0000	.0000	.4075
20	.0000	.0000	.0000	.0000	.0000	.0000	.4795
25	.0000	.0000	.0000	.0000	.0000	.0000	.4658
30	.0000	.0000	.0000	.0000	.0000	.0000	.4153
35	.0000	.0000	.0001	.0000	.0000	.0001	.4364
40	.0000	.0000	.0002	.0000	.0000	.0004	.3956
45	.0000	.0000	.0004	.0000	.0000	.0006	.4378
50	.0000	.0000	.0005	.0000	.0000	.0013	.3766
55	.0000	.0000	.0007	.0000	.0000	.0035	.2898
60	.0000	.0000	.0011	.0000	.0000	.0108	.2132
65	.0000	.0000	.0015	.0000	.0000	.0097	.2573
70	.0000	.0000	.0024	.0000	.0000	.0143	.2527
75	.0000	.0000	.0038	.0000	.0000	.0133	.3122
80	.0000	.0000	.0047	.0000	.0000	.0294	.2304
85	.0000	.0000	.0058	.0000	.0000	.0513	.1785
90	.0000	.0000	.0071	.0000	.0000	.0383	.2387
95	.0000	.0000	.0086	.0000	.0000	.1091	.1205
100	.0000	.0000	.0117	.0000	.0000	.1179	.1352

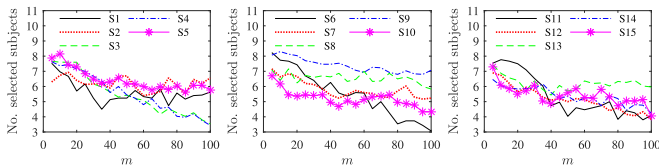


Fig. 6. Average number of similar subjects selected by SDS.

procedure [8], [9] were used to determine if the difference between any pair of algorithms was statistically significant, with a p -value correction using the false discovery rate method [2]. The p -values are given in Table I, where the statistically significant ones are marked in bold. Observe that the differences between OwARR and the other three algorithms (BL1, BL2, and DAMF) were always statistically significant when $m > 0$, so were the differences between OwARR-SDS and the two baseline algorithms. The difference between OwARR-SDS and DAMF was statistically significant for $m \in [5, 75]$. There was no statistically significant difference between OwARR and OwARR-SDS.

Finally, we can conclude that given the same amount of subject-specific calibration data, OwARR and OwARR-SDS can achieve significantly better estimation performance than the other three approaches. Or, in other words, given a desired RMSE, OwARR, and OwARR-SDS require significantly less subject-specific calibration data than the other three approaches. For example, in Fig. 4(a), the average RMSE for BL2 when $m = 100$ was 0.2988, whereas OwARR and OwARR-SDS can achieve even smaller RMSEs without using any subject-specific calibration samples. The average RMSEs for OwARR and OwARR-SDS when $m = 5$ were 0.2347 and 0.2348, respectively, whereas DAMF needed at least 45 subject-specific

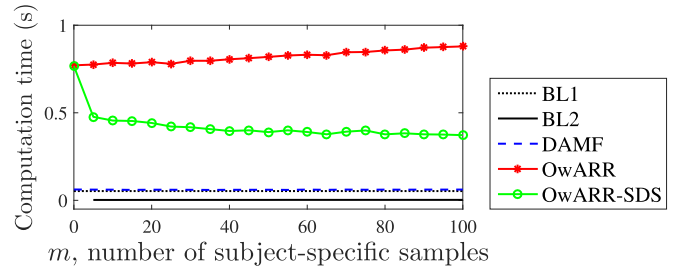


Fig. 7. Average training time of the five algorithms. Note that BL1 overlaps with DAMF.

samples to achieve these RMSEs, and BL2 needed at least 100 samples.

F. Computational Cost

In this section, we compare the computational cost of the five algorithms, particularly, OwARR and OwARR-SDS, because the primary goal of SDS is to downselect the number of auxiliary subjects and hence to reduce the computational cost of OwARR.

Fig. 6 shows the average number of similar subjects selected by SDS for the 15 subjects. Observe that most of the time fewer than seven subjects (half of the number of auxiliary subjects) were selected.

To quantify the computational cost of the five algorithms, we show in Fig. 7 the training times for different m , averaged over 10 runs and across the 15 subjects. The platform was a Dell XPS 13 notebook, with Intel Core i7-5500M CPU@2.40 GHz, 8 GB memory, and 256 GB solid-state drive. The software was MATLAB R2015b running in 64-bit Windows 10 Pro. Each algorithm was optimized to the best ability of the authors. Observe that the training time of BL1, BL2, and DAMF was

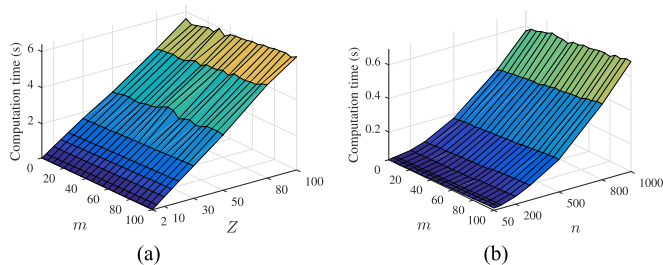


Fig. 8. Scalability of OwARR with respect to (a) number of source domains (each domain had about 1,200 samples) and (b) number of samples in each source domain (14 source domains were used).

almost constant, whereas the training time of OwARR increased monotonically as m increased. Interestingly, the training time of OwARR-SDS decreased slightly as m increased, because Fig. 6 shows that generally the average number of similar subjects selected by SDS decreased as m increased.

The computational costs of OwARR and OwARR-SDS were much higher than DAMF, because they used more sophisticated DA approaches. However, except for $m = 0$, at which point OwARR and OwARR-SDS had identical training time, the training time of OwARR-SDS was on average only about 49% of OwARR. This 51% computation time saving is very worthwhile when the number of source domains is very large and hence computing OwARR for all the source domains is too slow.

We also investigated the scalability of OwARR with respect to Z the number of source domains, and n the number of samples in each source domain. Because we only had 14 source domains in this dataset, we bootstrapped them to create additional domains when $Z \geq 14$. The results are shown in Fig. 8. Observe from Fig. 8(a) that the computational cost of OwARR increased linearly with the number of source domains, which is intuitive, because OwARR performs DA for each source domain separately and then aggregates the results. However, Fig. 8(b) shows that the computational cost of OwARR increased superlinearly with the number of samples in the source domains. Least-squares curve fitting found that the computation time was about $0.0000021 \cdot n^{1.8} + 0.035$ s, i.e., the computational cost is $O(n^{1.8})$ for 14 source domains.

Finally, it is important to note that the above analyses are only for the training of the algorithms. Once the training is done, the resulting OwARR and OwARR-SDS models can be executed much faster.

G. Robustness to Noises

It is also important to study the robustness of the five algorithms to noises. According to Zhu and Wu [68], there are two types of noises: *class noise*, which is the noise on the model outputs, and *attribute noise*, which is the noise on the model inputs. In this section we focus on the attribute noise.

As mentioned in [68], for each model input, we randomly replaced $q\%$ ($q = 0, 10, \dots, 50$) of all epochs from the new subject with a uniform noise between its minimum and maximum values. After this was done for both the training and

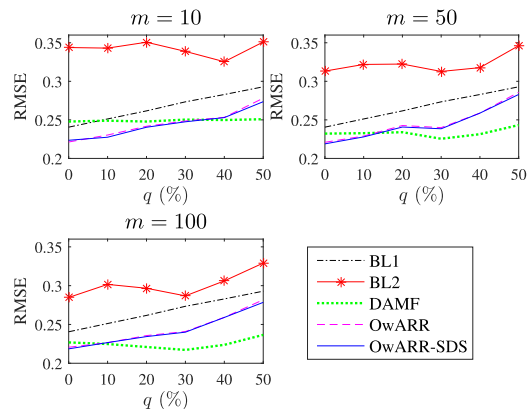


Fig. 9. Average RMSEs of the five algorithms with respect to different attribute noise levels.

testing data, we trained the five algorithms on the corrupted training data and then tested their performances on the corrupted testing data. The RMSEs for three different m (the number of labeled subject-specific samples), averaged across 15 subjects with 5 runs per subject, are shown in Fig. 9. Observe that as the noise level q increased, generally all algorithms had worse RMSEs. OwARR and OwARR-SDS still had the smallest RMSEs among the five when q was small. However, when q increased, DAMF became the best. This suggests that OwARR and OwARR-SDS may not be as robust as DAMF with respect to attribute noises, but when the noise level is low, the performance improvement achieved from the sophisticated optimizations in OwARR and OwARR-SDS dominates, and hence they are still the best algorithms among the five. When the noise level is high, we may need some noise handling approaches, e.g., noise correction [68], before applying OwARR and OwARR-SDS.

H. Parameter Sensitivity Analysis

The OwARR algorithm has three adjustable parameters: σ , which determines the weight w^t for the target domain samples; λ , which is a regularization parameter minimizing the distances between the marginal and conditional probability distributions in the source and target domains; and γ , which maximizes the approximate Pearson correlation coefficient between the true and estimated outputs. It is interesting to study whether all of them are necessary.

For this purpose, we constructed three modified versions of the OwARR algorithms by setting σ , λ , and γ to zero, respectively, and compared their average RMSEs with that of the original OwARR. The results are shown in Fig. 10. Observe that the original OwARR had better performance than all three modified versions, suggesting that all three parameters in OwARR contributed to its superior performance.

Next, we studied the sensitivity of OwARR to the three adjustable parameters, σ , λ , and γ . The results are shown in Fig. 11(a)–(c). Observe that OwARR is robust to σ in the range of $[0.1, 0.4]$, to λ in the range of $[1, 20]$, and to γ in the range of $[0.01, 1]$.

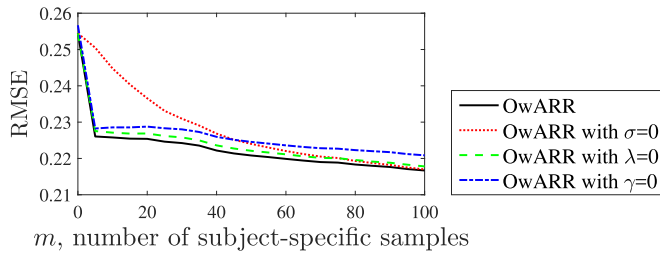


Fig. 10. Average RMSEs of OwARR when different regularization terms are removed.

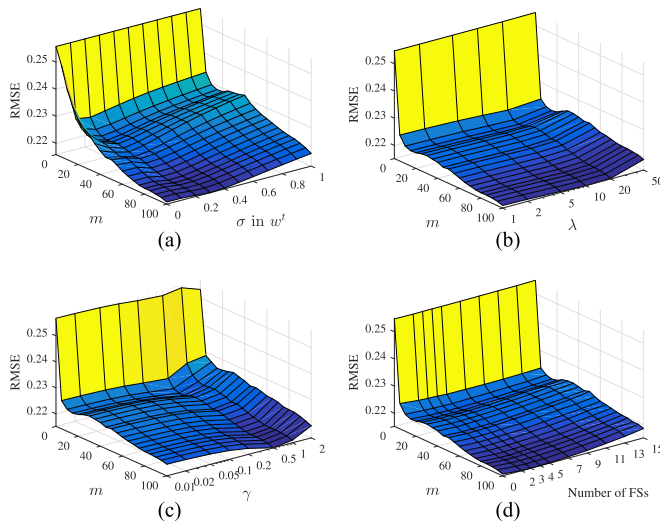


Fig. 11. Average RMSEs of OwARR across the 15 subjects for different parameter values. (a) σ in w^t ; (b) λ ; (c) γ ; (d) number of FSs in conditional probability distribution adaptation.

Additionally, three type-1 triangular FSs have been used in conditional probability distribution adaptation (see Section II-E) in this paper for simplicity. It is also interesting to study the sensitivity of the OwARR algorithm to the number of FSs. The results are shown in Fig. 11(d). Observe that OwARR gives the optimal performance when the number of FSs is between 2 and 5, but its performance gradually deteriorates when the number of FSs further increases. This is intuitive, because the target domain has a limited number of labeled training samples, so as the number of FSs increases, the number of target domain samples that fall into each fuzzy class decreases, and hence the computed fuzzy class means are less reliable. As a result, the distance between the conditional probability distributions [see (14)] cannot be reliably computed.

Another interesting question is that what would be the performance of OwARR if no FSs are used at all, i.e., conditional probability distribution adaptation is disabled? This is corresponding to the left-most slice in Fig. 11(d), where the number of FSs is zero. Observe that this results in worse RMSEs than the case that two to five FSs are used in conditional probability distribution adaptation, suggesting the FS approach is beneficial.

I. Effectiveness of the Ensemble Fusion Strategy

From Algorithm 1 (Algorithm 2) it is clear that the final step of OwARR (OwARR-SDS) uses ensemble learning: the

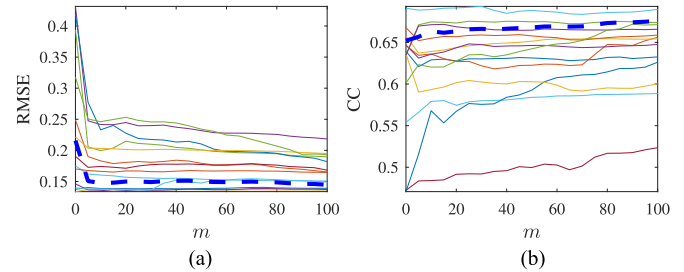


Fig. 12. Performances of the 14 base DA models (solid curves) and the final regression model (dashed blue curve) for a typical subject.

base DA models are aggregated using a weighted average to obtain the final regression model, and the weight is inversely proportional to the training RMSE of the corresponding base DA model. In this section, we study whether this fusion strategy is effective. The performances of the 14 base DA models and the final aggregation model for a typical subject are shown in Fig. 12. Observe that the aggregated model is better than most base DA models, and is also close to the best base DA model (which is unknown in practice), suggesting that the fusion strategy is effective. However, it may be possible that a better fusion strategy can make the final model outperform all base DA models. This will be one of our future research directions.

V. CONCLUSION AND FUTURE RESEARCH

TL, which improves learning performance in a new task by leveraging data or knowledge from other relevant tasks, represents a promising solution for handling individual differences in BCI. Previously we have proposed a wAR algorithm [59], [61] for offline BCI classification problems, an OwAR algorithm [60] for online BCI classification problems, and an SDS approach [60], [61] to reduce the computational cost of wAR and OwAR. In this paper, we have proposed an OwARR algorithm to extend the OwAR algorithm from classification to regression, and validated its performance on online estimation of driver drowsiness from EEG signals. Meanwhile, we have also extended the SDS algorithm for classification mentioned in [60] to regression problems, and verified that OwARR-SDS can achieve similar performance to OwARR, but save about half of the computation time. Both OwARR and OwARR-SDS use FSs to perform part of the adaptation regularization, and OwARR-SDS also uses FSs to select the closest source domains.

Although OwARR and OwARR-SDS have demonstrated outstanding performance, they can be enhanced in a number of ways, which will be considered in our future research. First, Fig. 5(a) shows that OwARR and OwARR-SDS had worse RMSEs than BL1 for some subjects. This indicates that they still have room for improvement: we could develop a mechanism to switch between BL1 and OwARR (OwARR-SDS) so that a more appropriate method is chosen according to the characteristics of the new subject, similar to the idea of selective TL [51]. Second, we will extend OwARR and OwARR-SDS to offline calibration, where the goal is to automatically label some initially unlabeled subject-specific samples with a small number of queries [61]. Semisupervised learning can be used

here to enhance the learning performance. Third, in this paper we combine the base learners using a simple weighted average, where the weights of the base learners are inversely proportional to their corresponding training RMSEs. This may not be optimal because what really matter here are the testing RMSEs. In online calibration, it is not easy to estimate the testing RMSEs because we do not know what samples will be encountered in the future; however, in offline calibration, we can better estimate the testing performances of the base learners using a spectral meta-learner approach [58], and hence a better model fusion strategy could be developed. Fourth, similar to offline classification problems [29], [55], [59], in offline regression problems, we can also integrate DA with active learning [40], [57] to further reduce the offline calibration effort. Finally, we will apply the online and offline DA algorithms to other regression problems in BCI and beyond to cope with individual differences, e.g., estimating the continuous values of arousal, valence, and dominance from speech signals [64] in affective computing.

ACKNOWLEDGMENT

The views and the conclusions contained in this document are those of the authors and should not be interpreted as representing the official policies, either expressed or implied, of the U.S. Army Research Laboratory or the U.S Government.

APPENDIX FUZZY SETS

FS theory was first introduced by Zadeh [67] in 1965 and has been successfully used in many areas, including modeling and control [49], [65], data mining [35], [62], [66], time-series prediction [14], [46], decision making [30], [31], [37], etc.

An FS X is comprised of a *universe of discourse* D_X of real numbers together with a *membership function* $\mu_X : D_X \rightarrow [0, 1]$, i.e.,

$$X = \int_{D_X} \mu_X(x)/x. \quad (24)$$

where \int denotes the collection of all points $x \in D_X$ with associated *membership degree* $\mu_X(x)$. An example of an FS is shown in Fig. 13. The membership degrees are $\mu_X(1) = 0$, $\mu_X(3) = 0.5$, $\mu_X(5) = 1$, $\mu_X(6) = 0.8$, and $\mu_X(10) = 0$. Observe that this is different from traditional (binary) sets, where each element can only belong to a set completely (i.e., with membership degree 1), or does not belong to it at all (i.e., with membership degree 0); there is nothing in between (i.e., with membership degree 0.5).

FSs are frequently used in modeling concepts in natural language, which may not have clear boundary. For example, we may define a *hot* day as temperature equal to or above 30°C , but is 29°C hot? If we represent *hot* as a binary set $\{x|x \geq 30\}$, then 29°C is not hot, because it does not belong to the binary set *hot*. However, this does not completely agree with people's intuition: 29°C is very close to 30°C , and hence it is somewhat hot. If we represent *hot* as an FS, we may say 29°C is hot with a membership degree of 0.9, which sounds more reasonable.

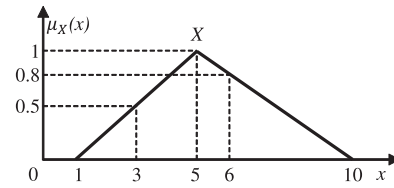
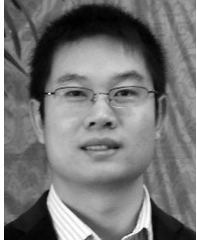


Fig. 13. Example of an FS.

REFERENCES

- [1] A. Bamdadian, C. Guan, K. K. Ang, and J. Xu, "Improving session-to-session transfer performance of motor imagery-based BCI using adaptive extreme learning machine," in *Proc. 35th Annu. Int. Conf. IEEE Eng. Med. Biol. Soc.*, Osaka, Japan, Jul. 2013, pp. 2188–2191.
- [2] Y. Benjamini and Y. Hochberg, "Controlling the false discovery rate: A practical and powerful approach to multiple testing," *J. Roy. Statist. Soc. Ser. B, Methodological*, vol. 57, pp. 289–300, 1995.
- [3] C.-H. Chuang, L.-W. Ko, T.-P. Jung, and C.-T. Lin, "Kinesthesia in a sustained-attention driving task," *Neuroimage*, vol. 91, pp. 187–202, 2014.
- [4] S.-W. Chuang, L.-W. Ko, Y.-P. Lin, R.-S. Huang, T.-P. Jung, and C.-T. Lin, "Co-modulatory spectral changes in independent brain processes are correlated with task performance," *Neuroimage*, vol. 62, pp. 1469–1477, 2012.
- [5] D. Coyle, G. Prasad, and T. McGinnity, "Faster self-organizing fuzzy neural network training and a hyperparameter analysis for a brain–computer interface," *IEEE Trans. Syst., Man, Cybern., B, Cybern.*, vol. 39, no. 6, pp. 1458–1471, Dec. 2009.
- [6] A. Delorme and S. Makeig, "EEGLAB: An open source toolbox for analysis of single-trial EEG dynamics including independent component analysis," *J. Neurosci. Methods*, vol. 134, pp. 9–21, 2004.
- [7] D. Devlaminck, B. Wyns, M. Grosse-Wentrup, G. Otte, and P. Santens, "Multisubject learning for common spatial patterns in motor-imagery BCI," *Comput. Intell. Neurosci.*, vol. 20, no. 8, 2011, Article no. 217987.
- [8] O. Dunn, "Multiple comparisons among means," *J. Amer. Statist. Assoc.*, vol. 56, pp. 62–64, 1961.
- [9] O. Dunn, "Multiple comparisons using rank sums," *Technometrics*, vol. 6, pp. 214–252, 1964.
- [10] T. Hastie, R. Tibshirani, and J. Friedman, *The Elements of Statistical Learning*. New York, NY, USA: Springer, 2009.
- [11] W.-Y. Hsu, "Unsupervised fuzzy c-means clustering for motor imagery EEG recognition," *Int. J. Innovative Comput. Inf. Control*, vol. 7, no. 8, pp. 4965–4976, 2011.
- [12] V. Jayaram, M. Alamgir, Y. Altun, B. Scholkopf, and M. Grosse-Wentrup, "Transfer learning in brain–computer interfaces," *IEEE Comput. Intell. Mag.*, vol. 11, no. 1, pp. 20–31, Feb. 2016.
- [13] H. Kang, Y. Nam, and S. Choi, "Composite common spatial pattern for subject-to-subject transfer," *Signal Process. Lett.*, vol. 16, no. 8, pp. 683–686, 2009.
- [14] N. K. Kasabov and Q. Song, "DENFIS: Dynamic evolving neural-fuzzy inference system and its application for time-series prediction," *IEEE Trans. Fuzzy Syst.*, vol. 10, no. 2, pp. 144–154, Apr. 2002.
- [15] R. Khushaba, S. Kodagoda, S. Lal, and G. Dissanayake, "Driver drowsiness classification using fuzzy wavelet-packet-based feature-extraction algorithm," *IEEE Trans. Biomed. Eng.*, vol. 58, no. 1, pp. 121–131, Jan. 2011.
- [16] G. J. Klir and B. Yuan, *Fuzzy Sets and Fuzzy Logic: Theory and Applications*. Upper Saddle River, NJ, USA: Prentice-Hall, 1995.
- [17] R. Koenker, *Quantile Regression*. Cambridge, U.K.: Cambridge Univ. Press, 2005.
- [18] B. J. Lance, S. E. Kerick, A. J. Ries, K. S. Oie, and K. McDowell, "Brain-computer interface technologies in the coming decades," *Proc. IEEE*, vol. 100, no. 3, pp. 1585–1599, May 2012.
- [19] Y. Li, H. Kambara, Y. Koike, and M. Sugiyama, "Application of covariate shift adaptation techniques in brain–computer interfaces," *IEEE Trans. Biomed. Eng.*, vol. 57, no. 6, pp. 1318–1324, Jun. 2010.
- [20] Y. Li, Y. Koike, and M. Sugiyama, "A framework of adaptive brain computer interfaces," in *Proc. 2nd IEEE Int. Conf. Biomed. Eng. Inf.*, Tianjin, China, Oct. 2009, pp. 1–5.
- [21] L.-D. Liao, "Biosensor technologies for augmented brain-computer interfaces in the next decades," *Proc. IEEE*, vol. 100, no. 2, pp. 1553–1566, May 2012.

- [22] C.-T. Lin, "Adaptive EEG-based alertness estimation system by using ICA-based fuzzy neural networks," *IEEE Trans. Circuits Syst. I, Reg. Paper*, vol. 53, no. 11, pp. 2469–2476, Nov. 2006.
- [23] M. Long, J. Wang, G. Ding, S. J. Pan, and P. S. Yu, "Adaptation regularization: A general framework for transfer learning," *IEEE Trans. Knowl. Data Eng.*, vol. 26, no. 5, pp. 1076–1089, May 2014.
- [24] F. Lotte, A. Lecuyer, and B. Arnaldi, "FuRIA: An inverse solution based feature extraction algorithm using fuzzy set theory for brain-computer interfaces," *IEEE Trans. Signal Process.*, vol. 57, no. 8, pp. 3253–3263, Aug. 2009.
- [25] F. Lotte, "Signal processing approaches to minimize or suppress calibration time in oscillatory activity-based brain-computer interfaces," *Proc. IEEE*, vol. 103, no. 6, pp. 871–890, Jun. 2015.
- [26] S. Makeig and M. Inlow, "Lapses in alertness: Coherence of fluctuations in performance and EEG spectrum," *Electroencephalogr. Clin. Neurophysiol.*, vol. 86, pp. 23–35, 1993.
- [27] S. Makeig and T. P. Jung, "Tonic, phasic and transient EEG correlates of auditory awareness in drowsiness," *Cogn. Brain Res.*, vol. 4, pp. 12–25, 1996.
- [28] S. Makeig, C. Kothe, T. Mullen, N. Bigdely-Shamlo, Z. Zhang, and K. Kreutz-Delgado, "Evolving signal processing for brain-computer interfaces," *Proc. IEEE*, vol. 100, no. Special Centennial Issue, pp. 1567–1584, May 2012.
- [29] A. Marathe, V. Lawhern, D. Wu, D. Slayback, and B. Lance, "Improved neural signal classification in a rapid serial visual presentation task using active learning," *IEEE Trans. Neural Syst. Rehabil. Eng.*, vol. 24, no. 3, pp. 333–343, Mar. 2016.
- [30] J. M. Mendel, *Uncertain Rule-Based Fuzzy Logic Systems: Introduction and New Directions*. Upper Saddle River, NJ, USA: Prentice-Hall, 2001.
- [31] J. M. Mendel and D. Wu, *Perceptual Computing: Aiding People in Making Subjective Judgments*. Hoboken, NJ, USA: Wiley, 2010.
- [32] C. Muhl, B. Allison, A. Nijholt, and G. Chanel, "A survey of affective brain computer interfaces: Principles, state-of-the-art, and challenges," *Brain-Comput. Interfaces*, vol. 1, no. 2, pp. 66–84, 2014.
- [33] R. Palaniappan, P. Raveendran, S. Nishida, and N. Saiwaki, "Evolutionary fuzzy ARTMAP for autoregressive model order selection and classification of EEG signals," in *Proc. IEEE Int. Conf. Syst., Man, Cybern.*, Nashville, TN, USA, Oct. 2000, vol. 5, pp. 3682–3686.
- [34] S. J. Pan and Q. Yang, "A survey on transfer learning," *IEEE Trans. Knowl. Data Eng.*, vol. 22, no. 10, pp. 1345–1359, Oct. 2010.
- [35] W. Pedrycz, "Fuzzy set technology in knowledge discovery," *Fuzzy Sets Syst.*, vol. 98, pp. 279–290, 1998.
- [36] B. Quanz and J. Huan, "Large margin transductive transfer learning," in *Proc. 18th ACM Conf. Inf. Knowl. Manage.*, Hong Kong, Nov. 2009, pp. 1327–1336.
- [37] C. C. Ragin, *Fuzzy-Set Social Science*. Chicago, IL, USA: Univ. Chicago Press, 2000.
- [38] F. Sagberg, P. Jackson, H.-P. Kruger, A. Muzer, and A. Williams, "Fatigue, sleepiness and reduced alertness as risk factors in driving," *Inst. Transport Econ., Oslo, Norway, Tech. Rep. TOI Rep. 739/2004*, 2004.
- [39] W. Samek, F. Meinecke, and K.-R. Muller, "Transferring subspaces between subjects in brain-computer interfacing," *IEEE Trans. Biomed. Eng.*, vol. 60, no. 8, pp. 2289–2298, Aug. 2013.
- [40] B. Settles, "Active learning literature survey," *Univ. Wisconsin-Madison, Comput. Sci. Tech. Rep. 1648*, 2009.
- [41] M. Spuler, W. Rosenstiel, and M. Bogdan, "Principal component based covariate shift adaption to reduce non-stationarity in a MEG-based brain-computer interface," *EURASIP J. Adv. Signal Process.*, vol. 2012, no. 1, pp. 1–7, 2012.
- [42] W. Tu and S. Sun, "Dynamical ensemble learning with model-friendly classifiers for domain adaptation," in *Proc. 21st Int. Conf. Pattern Recognit.*, Tsukuba, Japan, Nov. 2012, pp. 1181–1184.
- [43] W. Tu and S. Sun, "A subject transfer framework for EEG classification," *Neurocomputing*, vol. 82, pp. 109–116, 2012.
- [44] Traffic safety facts crash stats: Drowsy driving. *US Department of Transportation, National Highway Traffic Safety Administration*, Washington, DC, USA, 2011. [Online]. Available: <http://www-nrd.nhtsa.dot.gov/pubs/811449.pdf>
- [45] J. van Erp, F. Lotte, and M. Tangermann, "Brain-computer interfaces: Beyond medical applications," *Computer*, vol. 45, no. 4, pp. 26–34, 2012.
- [46] M. Versaci and F. C. Morabito, "Fuzzy time series approach for disruption prediction in Tokamak reactors," *IEEE Trans. Magn.*, vol. 39, no. 3, pp. 1503–1506, May 2003.
- [47] C. Vidaurre, M. Kawanabe, P. V. Bunau, B. Blankertz, and K. Muller, "Toward unsupervised adaptation of LDA for brain-computer interfaces," *IEEE Trans. Biomed. Eng.*, vol. 58, no. 3, pp. 587–597, Mar. 2011.
- [48] R. W. Walpole, R. H. Myers, A. Myers, and K. Ye, *Probability & Statistics for Engineers and Scientists*, 8th ed. Upper Saddle River, NJ, USA: Prentice-Hall, 2007.
- [49] L.-X. Wang, *A Course in Fuzzy Systems and Control*. Upper Saddle River, NJ, USA: Prentice-Hall, 1997.
- [50] P. Wang, J. Lu, B. Zhang, and Z. Tang, "A review on transfer learning for brain-computer interface classification," in *Prof. 5th Int. Conf. Inf. Sci. Technol.*, Changsha, China, Apr. 2015, pp. 315–322.
- [51] C.-S. Wei, Y.-P. Lin, Y.-T. Wang, T.-P. Jung, N. Bigdely-Shamlo, and C.-T. Lin, "Selective transfer learning for EEG-based drowsiness detection," in *Proc. IEEE Int. Conf. Syst., Man, Cybern.*, Hong Kong, Oct. 2015, pp. 3229–3232.
- [52] P. Welch, "The use of fast Fourier transform for the estimation of power spectra: A method based on time averaging over short, modified periodograms," *IEEE Trans. Audio Electroacoust.*, vol. 15, pp. 70–73, Jun. 1967.
- [53] J. Wolpaw and E. W. Wolpaw, Eds., *Brain-Computer Interfaces: Principles and Practice*. Oxford, UK: Oxford Univ. Press, 2012.
- [54] D. Wu, C.-H. Chuang, and C.-T. Lin, "Online driver's drowsiness estimation using domain adaptation with model fusion," in *Proc. Int. Conf. Affective Comput. Intell. Interact.*, Xi'an, China, Sep. 2015, pp. 904–910.
- [55] D. Wu, B. J. Lance, and V. J. Lawhern, "Active transfer learning for reducing calibration data in single-trial classification of visually-evoked potentials," in *Proc. IEEE Int. Conf. Syst., Man, Cybern.*, San Diego, CA, Oct. 2014, pp. 2801–2807.
- [56] D. Wu, B. J. Lance, and T. D. Parsons, "Collaborative filtering for brain-computer interaction using transfer learning and active class selection," *PLoS One*, vol. 8, 2013, Art. no. e56624.
- [57] D. Wu, V. J. Lawhern, S. Gordon, B. J. Lance, and C.-T. Lin, "Offline EEG-based driver drowsiness estimation using enhanced batch-mode active learning (EBMAL) for regression," presented at *IEEE Int. Conf. Syst., Man, Cybern.*, Budapest, Hungary, Oct. 2016.
- [58] D. Wu, V. J. Lawhern, S. Gordon, B. J. Lance, and C.-T. Lin, "Spectral meta-learner for regression (SMLR) model aggregation: Towards calibrationless brain-computer interface (BCI)," presented at *IEEE Int. Conf. Syst., Man, Cybern.*, Budapest, Hungary, Oct. 2016.
- [59] D. Wu, V. J. Lawhern, W. D. Hairston, and B. J. Lance, "Switching EEG headsets made easy: Reducing offline calibration effort using active weighted adaptation regularization," *IEEE Trans. Neural Syst. Rehabil. Eng.*, vol. 24, no. 11, pp. 1125–1137, Nov. 2016.
- [60] D. Wu, V. J. Lawhern, and B. J. Lance, "Reducing BCI calibration effort in RSVP tasks using online weighted adaptation regularization with source domain selection," in *Proc. Int. Conf. Affective Comput. Intell. Interact.*, Xi'an, China, Sep. 2015, pp. 567–573.
- [61] D. Wu, V. J. Lawhern, and B. J. Lance, "Reducing offline BCI calibration effort using weighted adaptation regularization with source domain selection," in *Proc. IEEE Int. Conf. Syst., Man, Cybern.*, Hong Kong, Oct. 2015, pp. 3209–3216.
- [62] D. Wu and J. M. Mendel, "Linguistic summarization using if-then rules and interval type-2 fuzzy sets," *IEEE Trans. Fuzzy Syst.*, vol. 19, no. 1, pp. 136–151, Feb. 2011.
- [63] D. Wu and T. D. Parsons, "Inductive transfer learning for handling individual differences in affective computing," in *Proc. 4th Int. Conf. Affective Comput. Intell. Interact.*, Memphis, TN, USA, Oct. 2011, vol. 2, pp. 142–151.
- [64] D. Wu, T. D. Parsons, E. Mower, and S. S. Narayanan, "Speech emotion estimation in 3D space," in *Proc. IEEE Int. Conf. Multimedia Expo.*, Singapore, Jul. 2010, pp. 737–742.
- [65] D. Wu and W. W. Tan, "Genetic learning and performance evaluation of type-2 fuzzy logic controllers," *Eng. Appl. Artif. Intell.*, vol. 19, no. 8, pp. 829–841, 2006.
- [66] R. Yager, "Database discovery using fuzzy sets," *Int. J. Intell. Syst.*, vol. 11, pp. 691–712, 1996.
- [67] L. A. Zadeh, "Fuzzy sets," *Inf. Control*, vol. 8, pp. 338–353, 1965.
- [68] X. Zhu and X. Wu, "Class noise vs. attribute noise: A quantitative study of their impacts," *Artif. Intell. Rev.*, vol. 22, pp. 177–210, 2004.



Dongrui Wu (S'05–M'09–SM'14) received the B.E. degree in automatic control from the University of Science and Technology of China, Hefei, China, in 2003, the M.Eng. degree in electrical engineering from the National University of Singapore, Singapore, in 2005, and the Ph.D. degree in electrical engineering from the University of Southern California, Los Angeles, CA, USA, in 2009.

He was a Lead Research Engineer at GE Global Research from 2010 to 2015. He is currently a Chief Scientist with DataNova, Clifton Park, NY, USA. His research interests include affective computing, brain–computer interface, computational intelligence, and machine learning. He has more than 80 publications, including a book entitled *Perceptual Computing* (Wiley-IEEE, 2010).

Dr. Wu received the IEEE International Conference on Fuzzy Systems Best Student Paper Award in 2005, the IEEE Computational Intelligence Society Outstanding Ph.D. Dissertation Award in 2012, the IEEE TRANSACTIONS ON FUZZY SYSTEMS Outstanding Paper Award in 2014, and the North American Fuzzy Information Processing Society Early Career Award in 2014. He was a selected participant of the first Heidelberg (Abel/Fields/Turing) Laureate Forum in 2013, the National Academy of Engineering German–American Frontiers of Engineering Symposium in 2015, and the 13th Annual National Academies Keck Futures Initiative Conference in 2015. He is an Associate Editor of the IEEE TRANSACTIONS ON FUZZY SYSTEMS, the IEEE TRANSACTIONS ON HUMAN–MACHINE SYSTEMS, and the IEEE COMPUTATIONAL INTELLIGENCE MAGAZINE.



Vernon J. Lawhern (M'16) received the B.S. degree in applied mathematics from the University of West Florida, Pensacola, FL, USA, in 2005, and the M.S. and Ph.D. degrees in statistics from the Florida State University, Tallahassee, FL, USA, in 2008 and 2011, respectively.

He is currently a Mathematical Statistician in the Human Research and Engineering Directorate, U.S. Army Research Laboratory, Adelphi, MD, USA. His current research interests include machine learning, statistical signal processing, and data mining of data collections for the development of improved

large neurophysiological brain–computer interfaces.



Stephen Gordon received the B.S. degrees in mechanical engineering in 2003 and electrical engineering in 2003 from Tennessee Technological University, Cookeville, TN, USA, the M.S. and Ph.D. degrees in electrical engineering from Vanderbilt University, Nashville, TN, USA, in 2005 and 2010, respectively.

He is currently a Research Engineer with DCS Corporation, Alexandria, VA, USA. He also works extensively in the area of brain–computer interfaces.

Since 2009, he has collaborated with researchers at the U.S. Army Research Laboratory Human Research and Engineering Directorate, on numerous projects and programs including the High-Definition Cognition ATO and the Cognition and Neuroergonomics Collaborative Technology Alliance. His research interests include signal processing and machine learning approaches for neurophysiological analysis and state detection.



Brent J. Lance (SM'14) received the Ph.D. degree in computer science from the University of Southern California (USC), Los Angeles, CA, USA, in 2008.

He was with USC's Institute for Creative Technologies as a Postdoctoral Researcher before joining Army Research Laboratory's Human Research and Engineering Directorate in 2010, where he currently a Research Scientist. He works on improving robustness of EEG-based brain–computer interaction through improved integration with autonomous systems. He has published more than 35 technical articles,

including a first-author publication on brain–computer interaction in the 100th anniversary edition of the PROCEEDINGS OF THE IEEE.

Dr. Lance is a member of the Association for Computing Machines.



Chin-Teng Lin (F'05) received the B.S. degree from the National Chiao-Tung University (NCTU), Hsinchu, Taiwan, in 1986 and the Master's and Ph.D. degrees in electrical engineering from Purdue University, West Lafayette, IN, USA in 1989 and 1992, respectively.

He is currently the Distinguished Professor of the Faculty of Engineering and Information Technology, University of Technology Sydney, Sydney, NSW, Australia. He also holds the Honorary Chair Professorship of Electrical and Computer Engineering,

NCTU, the International Faculty of University of California, San-Diego, CA, USA, and Honorary Professorship of University of Nottingham, Nottingham, U.K. He is the coauthor of *Neural Fuzzy Systems* (Prentice-Hall, 1996), and the author of *Neural Fuzzy Control Systems With Structure and Parameter Learning* (World Scientific, 1994). He has published more than 200 journal papers and holds 80 patents (H-index: 56) in the areas of computational intelligence, fuzzy neural networks, natural cognition, brain–computer interface, intelligent system, multimedia information processing, machine learning, robotics, and intelligent sensing and control, including approximately 105 IEEE journal papers.

Dr. Lin was elevated to be an IEEE Fellow for his contributions to biologically inspired information systems in 2005, and was elevated to an International Fuzzy Systems Association Fellow in 2012. He received the IEEE Fuzzy Systems Pioneer Award in 2016, the Outstanding Achievement Award by Asia Pacific Neural Network Assembly in 2013, the Outstanding Electrical and Computer Engineer Award, Purdue University, in 2011, and the Merit National Science Council Research Fellow Award, Taiwan, in 2009. He has been the Editor-in-Chief of the IEEE TRANSACTIONS ON FUZZY SYSTEMS since 2011. He also served on the Board of Governors at the IEEE Circuits and Systems (CAS) Society in 2005–2008, the IEEE Systems, Man, Cybernetics Society in 2003–2005, the IEEE Computational Intelligence Society (CIS) in 2008–2010, and the Chair of the IEEE Taipei Section in 2009–2010. He was the Distinguished Lecturer of the IEEE CAS Society from 2003 to 2005, and is currently the Distinguished Lecturer of the CIS Society from 2015–2017. He was the Deputy Editor-in-Chief of the IEEE TRANSACTIONS ON CIRCUITS AND SYSTEMS-II during 2006–2008. He was the Program Chair of the IEEE International Conference on Systems, Man, and Cybernetics in 2005 and the General Chair of the 2011 IEEE International Conference on Fuzzy Systems.